Developmental Biology 395 (2014) 154–166

Contents lists available at ScienceDirect

Developmental Biology

journal homepage: www.elsevier.com/locate/developmentalbiology

FGFR-ERK signaling is an essential component of tissue separation

Christian Hasse [a], Oliver Holz [a], Ellen Lange [a], Lisa Pisowodzki [a], Nicole Rebscher [a], Marie Christin Eder [b], Bert Hobmayer [b], Monika Hassel [a,*]

[a] Philipps-Universität Marburg, Faculty of Biology, Morphology and Evolution of Invertebrates, D-35039 Marburg, Germany
[b] C719, Institut für Zoologie, Technikerstraße 25, Victor Franz Hess Haus, A-6020 Innsbruck, Austria

ARTICLE INFO

Article history:
Received 24 March 2014
Received in revised form
28 July 2014
Accepted 10 August 2014
Available online 20 August 2014

Keywords:
Receptor tyrosine kinase
Autotomy
Actin cytoskeleton
Dominant-negative FGFR

ABSTRACT

Formation of a constriction and tissue separation between parent and young polyp is a hallmark of the *Hydra* budding process and controlled by fibroblast growth factor receptor (FGFR) signaling. Appearance of a cluster of cells positive for double phosphorylated ERK (dpERK) at the late separation site indicated that the RAS/MEK/ERK pathway might be a downstream target of the *Hydra* Kringelchen FGFR. In fact, inhibition of ERK phosphorylation by the MEK inhibitor U0126 reversibly delayed bud detachment and prevented formation of the dpERK-positive cell cluster indicating *de novo*-phosphorylation of ERK at the late bud base. In functional studies, a dominant-negative Kringelchen FGFR prevented bud detachment as well as appearance of the dpERK-positive cell cluster. Ectopic expression of full length Kringelchen, on the other hand, induced a localized rearrangement of the actin cytoskeleton at sites of constriction, localized ERK-phosphorylation and autotomy of the body column. Our data suggest a model in which (i) the *Hydra* FGFR targets, via an unknown pathway, the actin cytoskeleton to induce a constriction and (ii) FGFR activates MEK/ERK signaling at the late separation site to allow tissue separation.

Introduction

Fibroblast growth factor receptors originated in the common ancestor of Cnidaria and Bilateria (Rebscher et al., 2009). They control key functions in the development of all animals investigated so far like cell and tissue movement (Kadam et al., 2009; Klingseisen et al., 2009; Rottinger et al., 2008) boundary formation or branching morphogenesis (Affolter et al., 2009).

In the phylum Cnidaria, which separated from the main line of Metazoa early during evolution, FGFR signaling is essential during development and morphogenesis. Two FGFRs and two FGFs antagonistically control formation of the apical organ in the anthozoan *Nematostella* and target the MAPK pathway (Rentzsch et al., 2008). In *Hydra* at least one of two FGFRs (Rudolf et al., 2012) is required for proper detachment of a young polyp in the final phase of the budding process (Münder et al., 2010; Sudhop et al., 2004). Budding, the vegetative mode of propagation in *Hydra*, is enabled by mass tissue and cell movement from the parent body column to an evaginating bud, which also involves rearrangement of the extracellular matrix (Aufschnaiter et al., 2011). The molecular control mechanisms are just becoming elucidated. Bud initiation and evagination depends on canonical and noncanonical WNT signaling (Hobmayer et al., 2000; Philipp et al., 2009) with the extracellular matrix playing an essential role (Aufschnaiter et al., 2011).

While it became clear that the detachment process is initiated by FGFR signaling (Sudhop et al., 2004) and boundary formation is allowed by crosstalk of FGFR to Notch (Münder et al., 2010; Prexl et al., 2011), it is still obscure how tissue separation is controlled. To elucidate its mechanism, downstream targets of *Hydra* FGFR have to be identified.

FGFRs are canonically activated by binding of an FGF ligand and subsequent receptor-dimerisation, which activates the intracellular tyrosine kinase domain. Transphosphorylation of highly conserved tyrosine residues in the intracellular domain generates docking sites for intracellular binding proteins, which mediate coupling to signaling partners. Depending on cell type or stage mostly three alternatively used signaling pathways are targeted: PI/PKC signaling is activated by direct binding of PLC-γ to tyrosine-phosphorylated docking sites, activation of the RAS/MAP- kinase or the PI3-kinase pathways requires, in contrast, docking proteins (Lemmon and Schlessinger, 2010).

* Correspondence to: Philipps-Universität Marburg, FB 17, Morphology and Evolution of Invertebrates, Karl-von-Frisch-Str. 8, D-35032 Marburg, Germany.
E-mail addresses: ch.Hasse@web.de (C. Hasse), holzo@students.Uni-Marburg.DE (O. Holz), ellen.lange@biologie.uni-marburg.de (E. Lange), lisa.pisowodzki@t-online.de (L. Pisowodzki), rebscher@biologie.uni-marburg.de (N. Rebscher), Marie-Kristin.Eder@uibk.ac.at (M. Christin Eder), bert.hobmayer@uibk.ac.at (B. Hobmayer), Hassel@biologie.uni-marburg.de (M. Hassel).

http://dx.doi.org/10.1016/j.ydbio.2014.08.010
0012-1606/

In *Hydra*, analysis of the distribution and function of FGF ligands (Lange et al., in revision) and of downstream regulators like the branch suppressor Sprouty just started. Of the three alternative downstream pathways for FGFR signaling, neither PI/PKC signaling nor PI3-kinase are likely to be involved in budding as concluded from inhibitor experiments (Fabila et al., 2002). Activation of PI/PKC signaling by externally applied diacylglycerol or phorbol esters is known to strongly induce ectopic head formation along the body column and suppress budding, but effects on morphogenesis of existing buds have not been observed (Hassel et al., 1998; Müller, 1989). Inhibition of PI-3 kinase in *Hydra* upregulates apoptosis (David et al., 2005), without affecting bud morphogenesis (own unpublished observations). In early and mid bud stages CREB and MAPK signaling have been shown to be required for head formation (Fabila et al., 2002; Kaloulis et al., 2004; Manuel et al., 2006), but a role of MAPK in late budding has not been reported yet. Since the FGFR-dependent RAS/MAPK pathway is essential for morphogenesis in e.g. *Drosophila* (Mandal et al., 2004; Muha and Muller, 2013) we tested whether FGFR targets the RAS/MAPK signaling pathway in late budding stages. Our data indicate that FGFR-dependent activation of MEK and ERK are necessary to control the final steps of bud detachment and to complete tissue separation.

Material and methods

Polyps were kept at 18 °C with 16 h light, 8 h dark cycles in *Hydra* medium (0.29 mM $CaCl_2$, 0.59 mM $MgSO_4$, 0.5 mM $NaHCO_3$ and 0.08 mM K_2CO_3, pH 7.6) and fed five times a week to synchronize bud development (Sudhop et al., 2004). *Hydra vulgaris 1184 A*, a kind gift of Campbell and Steele, Irvine, was used for detection of dpERK in whole polyps, this strain allows a background-free detection of dpERK-stained cells. For all other experiments including transgenesis, *Hydra vulgaris AEP* was used. Since most of the previously described inhibitor experiments were done with *Hydra vulgaris Zürich* and since *H.v. AEP* is only distantly related to the Zürich strain (Hemmrich et al., 2007; Martínez et al., 2010), we repeated several experiments (inhibitor and regeneration) to ensure comparable responses.

Treatment with the MEK inhibitor U0126 and the FGFR inhibitor SU5402.

U0126 (CALBIOCHEM) inhibits MEK1 and MEK2 with an IC_{50} of 74 and 58 nM, respectively and acts highly specific. Stage 2–3 or stage 8–9 buds (Otto and Campbell, 1977) were selected and treatment started 4 h after the last feeding. Polyps were incubated at 18 °C in the dark for 24 h in *Hydra* medium containing 1% dimethylsulfoxide (DMSO), 1 mM adenosine triphosphate (ATP) and 10 μM each of U0126 (CALBIOCHEM) or SU5402 (SIGMA). These concentrations had been determined previously as optimal: above 15 μM both were increasingly toxic and animals disintegrated, below 5 μM less than 10% of the animals showed an effect. As controls we used both, normal animals or animals incubated in the DMSO/ATP solution, but omitting the inhibitor. Detachment of polyps was evaluated at the times indicated (usually at 24, 36, 48, 60, 72 and 96 h).

Statistical analysis

Inhibitor experiments were evaluated using a two tailed *t*-test for unequal variances. Percentage raw data were transformed into arcsine ($p' = \arcsin \sqrt{p}$) prior to the determination of mean and standard deviation in order to achieve a normal distribution (Zar, 2010). Mean and standard deviation were retransformed into percentage values. Using the *P*-values, statistical significance was finally encoded by asterisks in Fig. 3).

In situ hybridization

Whole-mount in situ hybridization was performed as described previously (Sudhop et al., 2004).

Western blot

The specificity of the dpERK antibody was verified in a Western Blot. Three *Hydra* polyps were boiled for 2 min in 25 μl of 2 × sample buffer containing a potent phosphatase inhibitor mix (PhosStop, ROCHE). Samples were quickly cooled on ice and subjected to denaturing PAGE. A Western blot was carried out following standard procedures on a PVDF membrane. The primary anti-dpERK antibody (mouse monoclonal anti-MAP kinase antibody (activated = diphosphorylated ERK-1/2), SIGMA-Aldrich) was used 1:200 diluted in PBS/0.1% Tween 20 with 5% bovine serum albumin (BSA fraction V). A single band was detected at about 45 kd using a peroxidase-coupled anti-mouse antibody and the ECL system (Pierce).

Immunohistochemistry against dpERK and DAPI staining of nuclei

Animals were relaxed at 18 °C in 2% urethane for 1 min. They were fixed for 2 h in 3.7% formaldehyde in 1 × PBS pH 7.0 including 50 mM ethylene glycol tetraacetic acid (EGTA) to block phosphatase activity. Polyps were washed and permeabilized 3 × 15 min in PBT (1x PBS with 0.15 M NaCl in 0.01 M sodium-phosphate buffer, pH 7.0 and 0.25% Triton X-100, v/v). Polyps were incubated for at least 2 h in blocking buffer (1 × PBT containing 2% BSA). The primary antibody (mouse monoclonal anti-MAP kinase (activated = diphosphorylated ERK-1&2), SIGMA-Aldrich) was incubated over night at 4 °C. For *Hydra vulgaris AEP* the primary antibody was diluted 1:20, for *Hydra vulgaris 1184A* 1:100 in blocking buffer. Following 6 × 20 min washing in PBT at room temperature, the specimens were incubated for 2 h at room temperature with the secondary antibody. For *H.v. AEP* we used the FITC-AffiniPure rabbit anti-mouse IgG (H + L), JACKSON ImmunoResearch, in a dilution of 1:200, for *Hydra vulgaris 1184A*, the anti-mouse-Cy3, SIGMA, diluted 1:500. As controls we used samples either without first or without second antibody. Unbound antibody was removed by 6 × 20 min washing steps in PBT and another washing step over night in PBS, pH 7.0 at 4 °C. To obtain nuclear staining, DAPI (SIGMA) was added to a final concentration of 0.5 μg/ml to the second of these washing steps. Specimen were embedded in Mowiol/DABCO and polymerized in the dark. For detection of dpERK in *Hydra vulgaris AEP* (Fig. 2) it was necessary to bleach their opaque tissue, which otherwise blurred the signal (Fig. S2). To this end *Hydra AEP* polyps were dehydrated prior to the blocking step in 25:75, 50:50, 70:30 MeOH:PBS and 100% MeOH for 5 min each and bleached in 80:20 MeOH:H_2O_2 for 1 h at 20 °C. Following rehydration in a MeOH:PBS series, and two washes in PBS, the above described protocol was continued starting with the blocking step. The bleaching step did not alter the dpERK distribution.

Single cell preparations were generated using a temperature-based method at neutral pH (Weber, 1995). In short, three *Hydra* were incubated for 10 min at 40 °C in 60 μl of dissociation medium (137 mM NaCl, 2.7 mM KCl, 10 mM Na_2HPO_4, 1.8 mM KH_2PO_4, pH 7.2 (PBS-K) containing 50 mM EGTA to conserve ERK phosphorylation. Cells were quickly cooled on ice, fixed in 4% formaldehyde for 10 min and spread on slides coated with 1 × Denhardt's solution (Sudhop et al., 2004). Thereby, they retain their typical shape almost perfectly. Immunohistochemistry, DAPI staining and embedding were performed as above for whole mount immunohistochemistry.

Staining was evaluated by fluorescence microscopy (Nikon TS2000 Eclipse) or cLSM (Leica TCS SP2 and SP5) and documented using digital photography.

Detection of F-actin by phalloidin staining

Animals were starved for at least 24 h. *Hydra* medium was replaced by 2% urethane in *Hydra* medium for 1 min and by ice cold 4% PFA (paraformaldehyde) in 1 × PBS for 1 h at 4 °C (50–100 rpm). Following three washes (10 min each) and permeabilization with 1 × PBS+0.1% Triton X-100 (PBT), the animals were washed three times for 5 min in 1 × PBTw (PBS+0.1% Tween 20). Incubation in 100 µl TRITC-Phalloidin (2.5 µM in PBTw, SIGMA) was for 1 h at 50 rpm. Three washes for 20 min each in 1 × PBTw were followed by an overnight washing step in 1 × PBS at 4 °C. Animals were embedded in Mowiol/DABCO and staining evaluated as described above.

Transgenesis and assignment of transgene to one of the epithelial layers

The pHot(G) vector (Wittlieb et al., 2006), which provides 5′ and 3′ actin regulatory sequences to drive GFP expression, was used to clone either the full length Kringelchen (*kring-GFP*) coding region or a sequence truncated at nucleotide 1308 (*kringΔ1308-GFP*), which removes the intracellular kinase domain. This truncation is known to yield a dominant-negative FGFR variant (Amaya et al., 1991).

Transgenic animals were established by microinjection of *Hydra* embryos as described (Wittlieb et al., 2006). In short, at least thousand *Hydra vulgaris AEP* were fed daily for several weeks. Sexual development was induced by feeding them only twice a week. Males were removed from the culture daily since they tend to overgrow the culture. When enough females with a single egg each had developed (at least 30 per day), eggs were fertilized by adding males. Subsequently one and two-cell stages were injected with the construct and the resulting embryos stored at 4 °C for 2 weeks to synchronize development. They hatched within another 14 days when moved to 18 °C, and about 16% of the hatchlings carried transgenic cells as evaluated by fluorescence microscopy to detect GFP. Although one- or two-cell stages were injected, *Hydra* expressed the transgene exclusively in a few cells of only one of the two epithelial layers (in this study. Others showed that integration in a single to all three stem cell lines: ecto-, ento-, and interstitial cells is possible (Khalturin et al., 2007)). Within the next weeks, hatchlings grew and the transgenic cells multiplied by proliferation. When the transgenic cells were located in the budding zone, they became exported (by intercalation) into a bud and formed a longitudinal stripe. Depending on the width of the stripe, one of the next buds was formed by transgenic cells, exclusively. Assignment of the transgene to one of the two single-layered epithelia (called ecto- or entoderm in *Hydra* throughout their life cycle) was possible by evaluating the GFP fluorescence in living polyps under the dissection microscope—transgenic cells were the either detected in the ectodermal single cell layer above the basal membrane or below it. Presence of the *kringΔ1308-GFP* or the full length *kring-GFP*, which are only weakly expressed in the polyp's gastric region was furthermore confirmed by PCR of genomic DNA isolated from a small *Hydra* tissue piece of each line.

Primer sequences used to generate the constructs and verify presence of the transgene:

pHotGkringfw: TTTTTGCTAGCATGATATCAGATTGGTGTGTTG, pHotGkringrv1308: TTTCCCGGGGGAAGCAGAGACAGAAGTAACC (truncated), pHotGkringrvfull: TTTCCCGGGAGAAACTGCATAGTGACTAAGAAG (full-length).

Results

The RAS/MEK/ERK pathway is a potential target of FGFR signaling. Indicative for its activation is the presence of double phosphorylated (activated) ERK (dpERK), which is generated in a series of phosphorylation events downstream of FGFR (op. cit. (Lemmon and Schlessinger, 2010)). Following ligand binding FGFR docks to proteins, which activate the GTPase RAS. RAS activates the serine-threonine kinase Raf1, which phosphorylates MEK. Finally, activated MEK phosphorylates ERK and generates its activated, double phosphorylated form, dpERK. The spatio-temporal activation of RAS/MEK/ERK signaling can thus be analyzed in whole tissue or single cells simply by immunohistochemistry against dpERK.

To investigate local ERK activation in *Hydra*, we used an antibody directed against double phosphorylated ERK1/2 (Thr 202/Tyr 204 in the highly conserved mouse epitope HTGFL**pT**E**pY**VAT). This epitope is conserved in the predicted single *Hydra* ERK (syn. MAPK3, NCBI reference XP_002164372.2, partial EST) with a single F/M amino acid exchange. In a Western blot the antibody detected a single band of 45 kd in *Hydra*, which corresponds to about the expected size of ERK (Fig. S1).

Cells positive for phosphorylated ERK are scattered throughout the Hydra body and the activated kinase is localized mostly in nuclei

In whole mount immunohistochemistry using the small and translucent *Hydra vulgaris 1184A*, the antibody detected dpERK-positive cells scattered throughout the body column including the terminally differentiated tentacles and basal disc (Fig. 1). This indicates that dpERK is not restricted to proliferating cells which are located in the gastric region and excluded from the terminally differentiated basal disk and tentacles (Holstein et al., 1991). The pattern was somewhat variable and ranged from animals with an almost even distribution of stained cells along the body column to animals, in which these cells formed zones of higher density in different body regions (Fig. 1(A), Fig. S2 (B), (E) and (G)). Consistently, a cluster of strongly stained cells was found at the late bud base (Fig. 1(A), (C)–(E) and Fig. S2(B), (D), (G), (H)). Presence of a dark spot within the stained structure (Fig. 1(C)) suggested that dpERK was either localized in small, roundish cells with an unstained nucleus- or in big nuclei with an unstained nucleolus. This issue was solved by evaluating a double staining for dpERK and the nuclear marker DAPI. The strong dpERK signal could clearly be assigned to nuclei (Fig. 1 (C), (D), (E) and see the magenta overlay staining in Fig. 1(M) and (U); overview in Fig. S2 (I)–(L) with either a single or two nucleoli (Fig. 2 (Q), (R)). In *Hydra*, two nucleoli are typical for subsets of epitheliomuscular cells and big interstitial stem cells (I-cells) as shown for epithelial cells in Fig. S4(C)). Of the I-cells about 40% remain stem cells and 60% proliferate as so-called small i-cells to give rise to neurons, nematocytes (stinging cells) and germ cells (David, 2012; Hobmayer et al., 2012). Because the cell types are difficult to distinguish in whole mounts, we gently dissociated whole *Hydra* with a short heat shock at neutral pH (Weber, 1995) to obtain single cells for DAPI and dpERK staining (Fig. 1(F)–(U)). In the cytoplasm of all cells, a low level of dpERK was detected (Fig. 1(G), (K), (O), (S)). Additionally, about 15% of the epitheliomuscular cells (19 of 160 cells counted) and about 20% of the I-cells (15 of 76 counted) showed a strong cytosolic and an additional nuclear staining indicated by the purple color in Fig. 1 (M) and (U) and in the overview of stained and unstained cells in Fig. S2(I)–(L)) Activated ERK was not detected in nuclei of small i-cells, which occur in nests of up to 32 differentiating cells (Fig. 1(N)–(Q) and Fig. S2). This result is in line with the data obtained in whole mounts, where nests of cells were not visible. We cannot exclude that the short heat shock required to dissociate *Hydra* causes side effects and alters dpERK localization or ERK phosphorylation levels, the more, since di-phosphorylated ERK has been shown to result from wounding (Chera et al., 2011). Despite this drawback, the presence of two nucleoli in some of the stained nuclei in the cluster at the bud base (Fig. 2(Q) and (R)) is consistent with the detection of nuclear dpERK in heat-dissociated epitheliomuscular and I-cells.

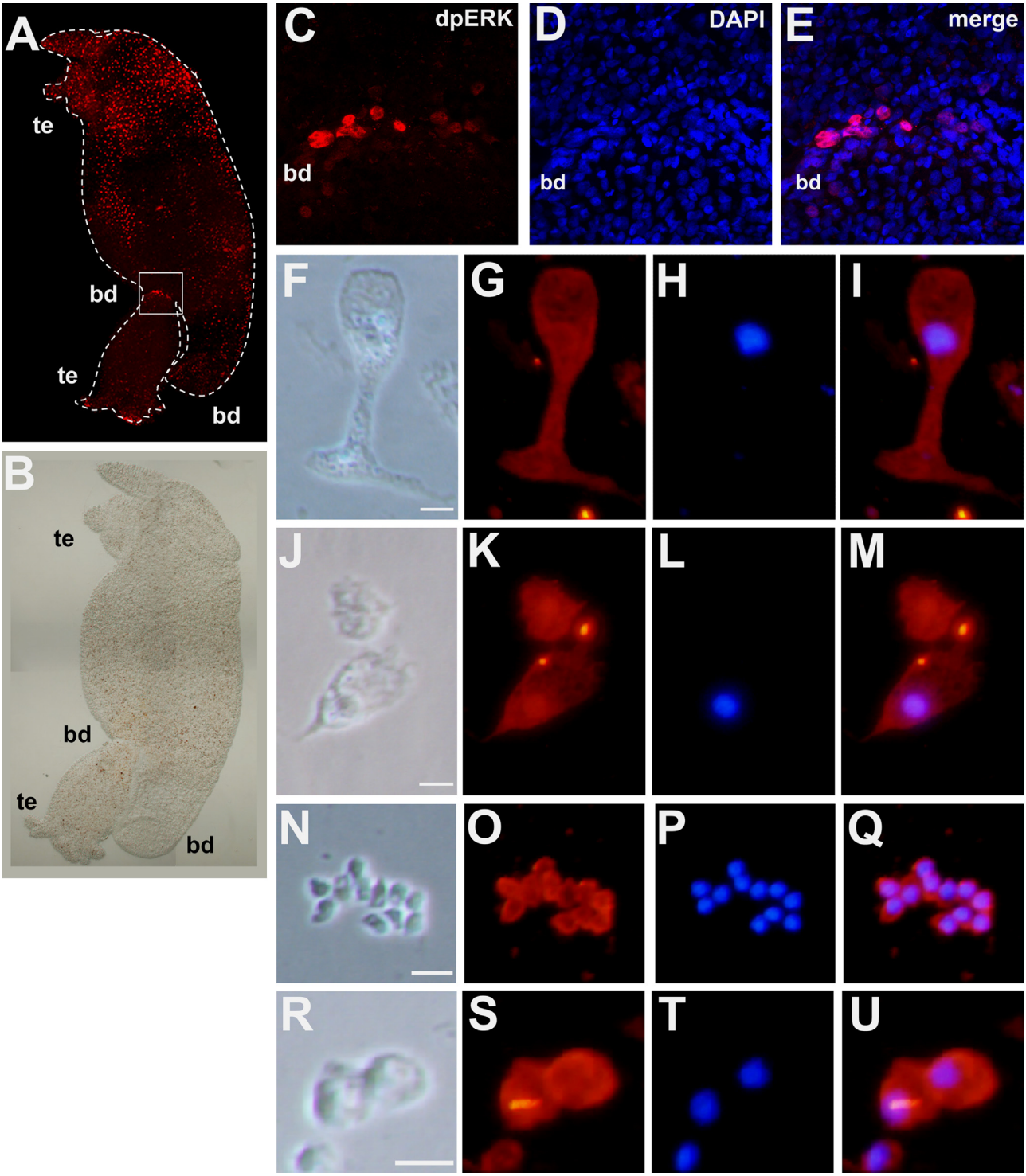

Fig. 1. Distribution of dpERK positive cells in *Hydra vulgaris 1184A* and identification of cell types and subcellular localization by single cell preparations. Activated ERK was detected using an anti-dpERK antibody (SIGMA) and a Cy3-coupled secondary antibody. (A) and (B) Overview of a whole polyp carrying a stage 8-9 bud. The dpERK-positive cells occur ectodermally in all body parts including the terminally differentiated tentacles (te) and basal disc (bd) of parent and bud. (C)–(E) Close-up of the cluster of dpERK-positive cells at the parent-bud boundary (box in (A)), (C) dpERK staining, (D) detection of nuclei by DAPI and (E) overlay to allow assignment of dpERK to nuclei. (F)–(U) Single cell preparations demonstrating in (F)–(I) an epithelial cell with no colocalization of dpERK and DAPI (blue overlay), (J)–(M) an epithelial cell in which dpERK and DAPI colocalize (magenta overlay), (N)–(Q) a nest of i-cells (no colocalization) and (R)–(U) big I cells (colocalization, magenta overlay). Size bar indicates 20 μm.

ERK phosphorylation is differentially regulated during budding

We next investigated in which phase of budding the cluster of dpERK-positive cells occurs. All further experiments were carried out with the *Hydra vulgaris AEP* strain to ensure comparability with the Kringelchen-transgenic *H.v. AEP* lines used later in this study (see below). Distribution of dpERK-positive cells is similar in *H.v. AEP* and *H.v. 1184A*, although more difficult to analyze in *Hydra AEP* (Fig. S2, compared to (B)–(D) to (E)–(H)).

In Fig. 2 *kringelchen* in situ hybridization and dpERK immunohistochemistry are presented side-by-side to reveal potential colocalization in budding polyps. Examples are given for the three

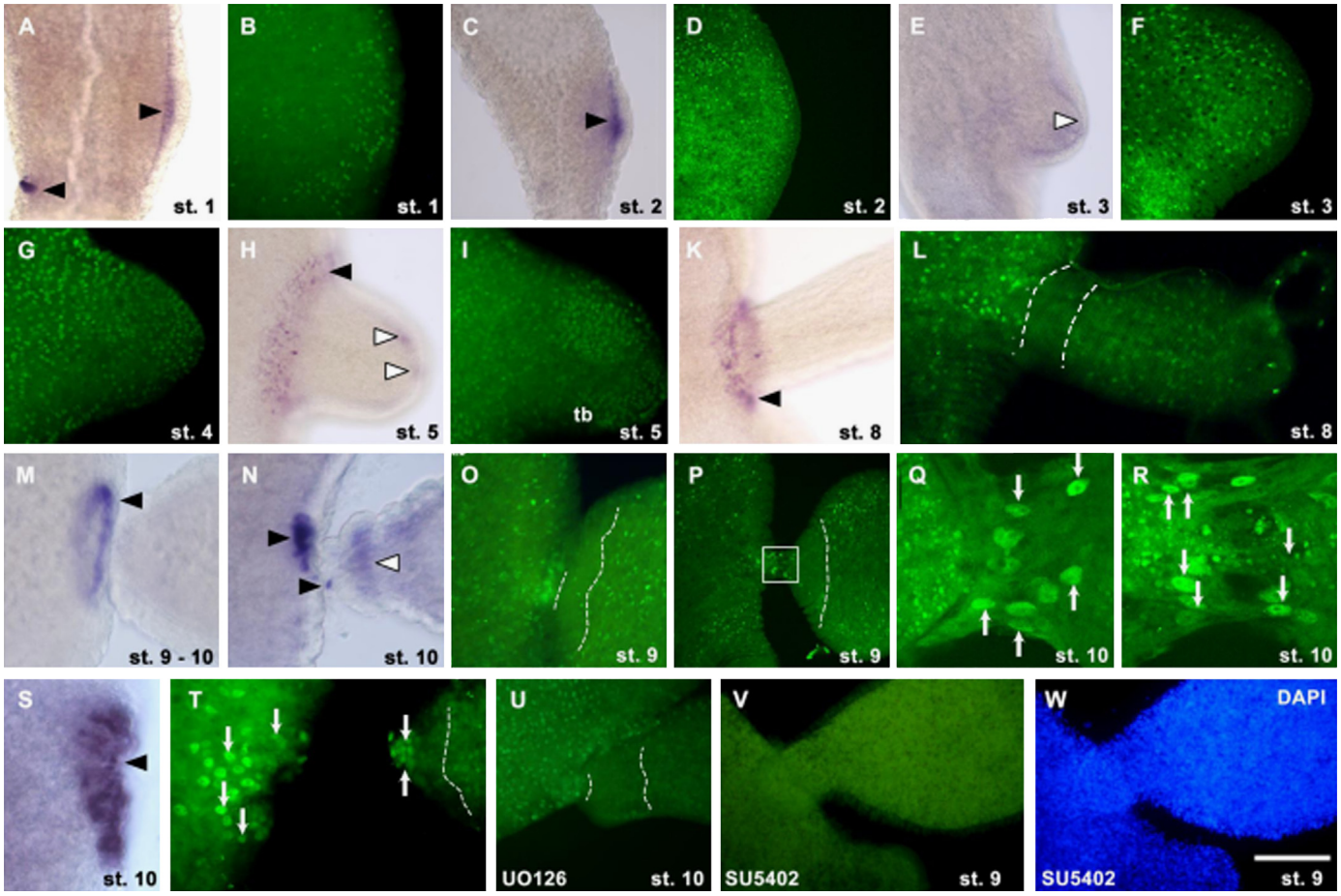

Fig. 2. Pattern of *kringelchen* expression and dpERK-positive cells in buds and of dpERK in U0126 or SU5402-treated buds. (A), (C), (E), (H), (K), (M), (N), (S) In situ hybridization with a *kringelchen* antisense probe, black arrowheads indicate ectodermal, white ones endodermal expression domains. The pictures in M, N and S were taken using differential interference contrast (DIC) optics. Activated ERK was detected using an anti-dpERK antibody and a FITC-coupled secondary antibody. The early ubiquitous salt-and-pepper pattern of dpERK in stages 1–4 is lost, when from stage 5 (I) a dpERK-free zone forms at the bud base (dotted lines in L,O,P, T, U) and persists until the bud detaches. (O), (P) and (T) dpERK-positive cluster of cells close to the bud base. (Q) and (R) Close-up of box in (P), arrows indicate dpERK-positive nuclei, the arrows indicate dpERK-labelled cells. (S) and (T) Potential colocalization of *kringelchen* mRNA and dpERK-positive cells in the tissue bridge between parent and stage 10 bud. (T) This bud was ripped off in stage 10. (U)–(W) Animals treated with either U0126 or SU5402 immediately after the end of treatment. (U) MEK-inhibitor U0126 treated stage 8 (U). The dotted line indicates the zone almost free of dpERK-positive cells, the cluster of dpERK-positive cells failed to form. (V) and (W) Treatment with SU5402 completely erased dpERK in any bud stage, shown is a stage 9 bud. (V) dpERK and (W) DAPI demonstrate lack of (nuclear) dpERK. All fluorescence pictures were taken at 330 msec. Abbreviations tb tentacle bud might be starting to emerge, but the ectoderm is still smooth. Size bar is 20 m.

main budding phases: evagination (Fig. 2(A) and (F)), elongation (Fig. 2(G) and (L)) and detachment (Fig. 2(M)–(T)). The three phases are further subdivided into ten bud stages (Otto and Campbell, 1977). (1) In the early evagination phase (bud stages 1–3) *kringelchen* is expressed ectodermally (Fig. 2(A) and (C)) and switches, from stage 3 onwards to the endoderm of the evaginating bud tip (Fig. 2(E)). Distinction of ecto- and entodermal staining in *Hydra* is possible by using the mesogloea (basal membrane) between the two single-layered epithelia as a reference. Stained cells and mesogloea are not always optimally visible in the same optical section, Fig. S4(A) and (B) gives an example for the assignment of ecto- and entoderm of the polyp shown in Fig. 2(C), in which the focus here is on the stained cells.

(2) In the elongation phase (bud stages 4–7) *kringelchen* expressing ectodermal cells form a ring at the bud-parent boundary. Through this ring, parental tissue constantly moves into the bud and transiently upregulates the gene (Fig. 2(H) and (K)). (3) In the detachment phase (stages 8–10), *kringelchen* is first expressed at high levels in an ectodermal ring of parental tissue surrounding the constriction zone between both polyps (Fig. 2(M)). Later, in stage 10, when the epithelia of parent and bud separate, *kringelchen* retracts to an ectodermal patch of parental cells expressing the gene at a high level (Fig. 2(N) and (S)). A transient weak upregulation of the FGFR mRNA was detected in the endoderm of the bud basal disc (Fig. 2(N)).

Comparison of the distribution of dpERK-positive cells to *kringelchen* expression reveals no correlation before stage 9. The density of cells carrying the activated ERK is indistinguishable in bud and parental tissue (Fig. 2(B), (D), (F), (G), and (I)). A tendency for more densely packed cells in the apical tip of evaginating buds (Fig. 2(G)) and tentacle buds (Fig. 2(I)) could not be corroborated. In stage 9, the cluster of dpERK-positive cells forms at the bud base (Fig. 2(O) and Fig. S2(G) and (H)).

Although dpERK and *kringelchen* are not colocalized up to stage 9, an interesting negative correlation was observed from late stage 5 to the end of detachment. Concomitant with the establishment of a *kringelchen*-positive ring at the bud-parent boundary (Fig. 2(K) and (M)), a belt of cells almost devoid of dpERK became visible immediately distal to the *kringelchen* expressing cells (indicated in Fig. 2(L), (O), (P), (T) and (U) by broken lines). This zone was not result of a reduced cell number as revealed by DAPI staining (compare Fig. 1(D) and (E)). Distal to this belt, dpERK-positive cells reappeared in a pattern corresponding to the parent body column (compare Figs. 1(L), (O) and (P) and S2(D) and (H)). Thus, ERK phosphorylation is shut down in previously *kringelchen*-positive cells, which move into the bud (Fig. 2(J) and (L)). It will be

interesting to analyze, whether these cells contain the Kringelchen protein as its preceding expression suggests.

In stage 10, strong ectodermal *kringelchen* expression in parental tissue correlates with the ectodermal cluster of dpERK-positive cells (compare Fig. 2(N) and (S) with (O) and (T)). The endodermal dpERK signal (Figs. 2(Q), (R) and S4(D)) might be due to unspecific trapping of the antibody: it was detectable in whole mounts of *H.v.* AEP only (not in single cell preparations) and could not be assigned to subcellular structures.

Ectodermal cells with dpERK-positive nuclei also appeared in the tissue bridge connecting bud and parent (Fig. 2(Q), (R)). Whether these cells actively migrate, are stationary and/or are passively transferred remains to be shown as well as whether the few solitary cells expressing the FGFR (Fig. 2(N), arrowhead) contain a dpERK-positive nucleus.

In summary, strong *kringelchen* expression in a patch of parental cells close to the late detachment site correlates with the appearance of dpERK in nuclei of a subset of these cells. This finding supports the hypothesis that FGFR signaling might target the RAS-MEK-ERK pathway.

The MEK inhibitor U0126 prevents appearance of dpERK-positive cells at the bud base and delays detachment

Provided FGFR signaling induces ERK phosphorylation and dpERK in turn is essential for bud detachment, pharmacological interference with either FGFR or with MEK should interfere with the last steps of budding.

Our previous study had shown that FGFR inhibition in stage 2–3 buds prevents formation of the constriction at the bud base ((Sudhop et al., 2004) and compare to Fig. S5(C)), but the effect of SU5402 on late bud stages had not been investigated. We therefore compared the impact of FGFR inhibition to that of MEK inhibition by U0126 in stage 2–3 buds as well as in stage 8–9 buds. As endpoints, we evaluated (1) bud morphology, (2) the distribution of dpERK-positive cells in early buds (not shown but similar to late buds for U0126), (3) the appearance of the dpERK-positive cluster in stage 10 and (4) the time required until all young polyps had detached (Fig. 3).

Conspicuous is that the solvent (1% DMSO, 1 mM ATP) delayed detachment by about 12 h (Figs. 3 and S3). Neither morphogenesis nor the appearance of the cluster of dpERK-positive cells were influenced. This delayed detachment is likely due to the permeabilising effects of both, DMSO and ATP (Cutaia et al., 1996; Sanmartin-Suarez et al., 2011), which on one hand is desired to transfer the small inhibitor molecules into the cells, but on the other hand might cause leakage of small molecules required for timely detachment.

The MEK inhibitor, U0126, did not influence bud morphology or the overall distribution of dpERK-positive cells in the body column of early or late buds. However, treatment of stage 8–9 buds, prevented formation of the cluster of dpERK-positive cells (Fig. 2(U)). This indicates a stable ERK phosphorylation in cells of the body column (not affected by the inhibitor) as well as ERK *de novo* phosphorylation by MEK at the bud base, which is now inhibited. U0126 also significantly delayed detachment of the buds (Fig. 3), and most of the treated young polyps detached only after 60 and 72 h compared to 48–60 h in the solvent control.

The FGFR inhibitor SU5402 strongly altered the morphology of buds treated in stage 2–3 as described previously for *Hydra vulgaris*, *Zürich* (Sudhop et al., 2004): formation of the constriction in stage 8 failed and the young polyp persisted as secondary axis (Fig. S5(C)–(E)). Since *Hydra vulgaris*, *Zürich* and *Hydra AEP* are distantly related (Hemmrich et al., 2007; Martínez et al., 2010), FGFR signaling is a canonical pathway required for normal bud morphogenesis in various *Hydra* strains.

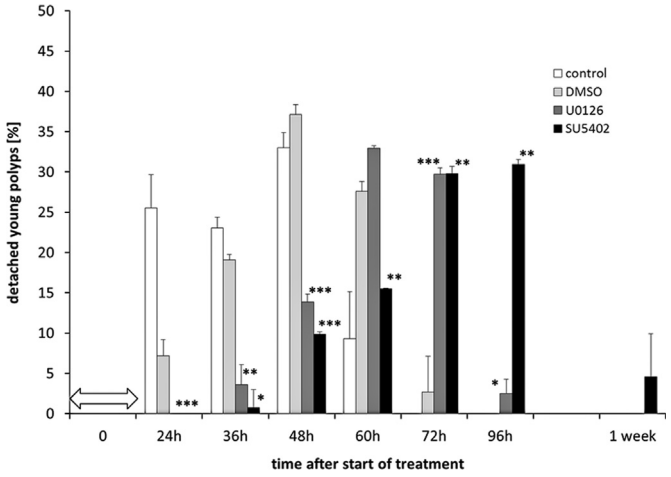

Fig. 3. Delay of bud detachment following treatment with the MEK inhibitor U0126 or the FGFR inhibitor SU5402. Polyps carrying a stage 9 bud were treated for 24 h (horizontal arrow) with the respective inhibitor and detached young polyps were counted at the given time points (U0126, dark gray columns; SU5402, black columns). Negative controls are *Hydra* medium (white columns) and the solute (1% DMSO, 1 mM ATP in hydra medium, light gray columns). Asterisks denote statistical significance at the level of 5% (*), 1% (**) and 0.1% (***), respectively, for solute versus inhibitor experiments. For additional details of the statistical analysis (*P*-values) refer to Fig. S3. Numbers of independent replicates with 20–30 animals per experiment were $n=9$ (medium control or solute), $n=6$ (U0126) and $n=3$ (SU5402), respectively. A two tailed *t*-test for unequal variances was carried out. Percentage raw data have been transformed into arcsine ($p'=\arcsin\sqrt{p}$) prior to the determination of mean and standard deviation in order to achieve a normal distribution (Zar, 2010). Mean and standard deviation were retransformed for this figure into percentage values.

In contrast to U0126, SU5402 caused the disappearance of dpERK throughout the body column (Fig. 2(V), and (W)). This result might indicate that SU5402 besides inhibiting tyrosine phosphorylation also increases phosphatase activity, an interesting starting point for future studies. Like U0126, SU5402 significantly delayed detachment when stage 9 polyps were treated: most of the young polyps detached only after 72 to 96 h and thus 24h later than comparable late buds treated with the MEK inhibitor (Fig. 3).

Taken together,the data indicate that FGFR signaling is essential from early stages to control bud morphogenesis (specifically formation of the constriction) and later for timely detachment. Unlike FGFR, MEK activity is not required for the establishment of a constriction, but essential for the late steps of tissue separation. Inhibition of either of these kinases in late bud stages correlates with the lack of formation of the dpERK-positive cluster, which likely forms by localized *de novo* phosphorylation of ERK through MEK. In both cases, the bud remains attached to the parent with a tiny tissue bridge. Therefore, this cluster of cells might provide factors, e.g. proteases to digest this bridge or e.g. peptides to contract the sphincter at the bud base, which allow tissue separation. Such markers have to be investigated in the future.

Dominant-negative Kringelchen prevents formation of the dpERK-positive cluster of cells and removal of the small tissue bridge between parent and bud

Since inhibitor treatment might have side effects, we asked whether a Kringelchen knockdown affects detachment and interferes with formation of the dpERK-positive cluster of cells. Dominant-negative FGFRs result from removal of the intracellular kinase domain as well as the SH2 and SH3 binding consensus sites (Amaya et al., 1991). They are able to bind FGF and to dimerize with the endogenous normal or with the mutant FGFR molecules. However, due to the lack of transphosphorylation, and thus docking sites for intracellular signaling partners, heterodimers as well

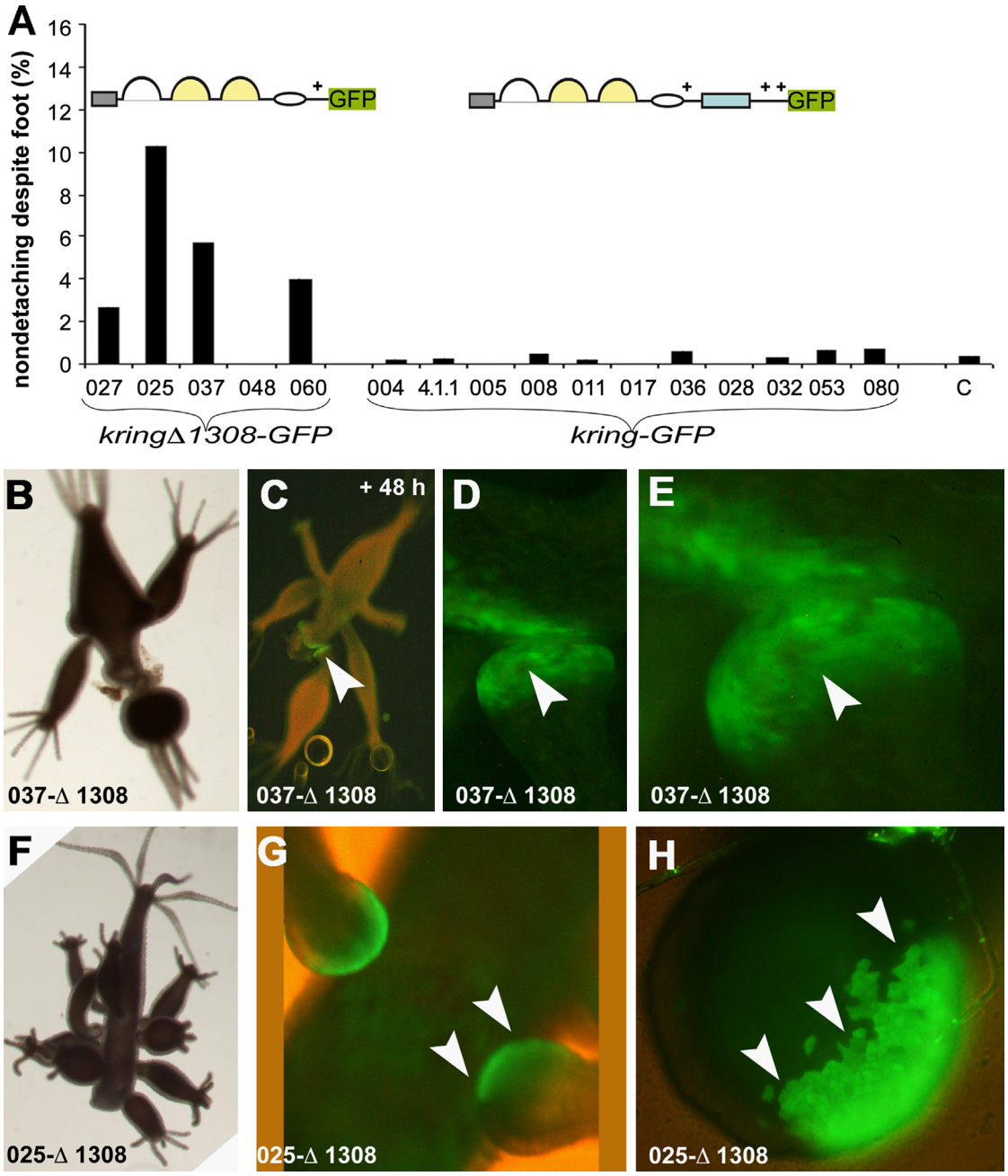

Fig. 4. *KringΔ1308-GFP* transgenic lines develop a phenotype of nondetaching buds despite formation of a basal disc. (A) Percentage of the nondetaching phenotype (despite differentiation of a basal disc) compared to *kring-GFP* lines overexpressing the full length Kringelchen FGFR. Evaluation was carried out bi-weekly over about one year. Of several hundred control animals (c) expressing GFP driven by the same regulatory sequences less than 1% developed this phenotype. Presence of the transgene was verified by PCR and life microscopy to detect GFP. (B)–(E) life imaging of line 037, (F)–(H) life imaging of line 025. (B) and (F) Colony-like phenotype resulting from the failure of bud detachment despite a fully formed foot (seen in (G) and (H)). (D) and (E) Close-up of the basal disc indicated by the arrowhead in (C). (G) and (H) Ectodermal localization of the transgene can clearly be seen, in (H) the partially transgenic basal disc is focused from below by inverse microscopy to detect single cells (arrowheads) carrying the transgene in the cytoplasm and cell membrane. Such partially transgenic basal discs allow detachment.

as the mutant homodimers prevent or attenuate signal transduction. Attenuation in this case depends on the presence of residual functional homodimers.

Using the approach described for vertebrate FGFR we generated the *kringΔ1308-GFP* fusion construct using a vector with *Hydra* actin regulatory sequences flanking GFP (Wittlieb et al., 2006). *kringΔ1308-GFP* lacks the sequences encoding the intracellular kinase and the two predicted C-terminal SH2 and SH3 binding site consensus sequences (Sudhop et al., 2004).

All five resulting transgenic *Hydra* lines (Fig. 4(A)) expressed the transgene weakly in ectodermal epithelial cells (GFP visible in the body column of Fig. 4(D) and mRNA in Fig. 5(D) between the two buds). Despite the constitutive actin promoter, the transgene was upregulated in the ectoderm of basal disc tissue as shown for lines 025-*kringΔ1308-GFP* and 037-*kringΔ1308-GFP* (Fig. 4(C), (D), (E), (G) and (H) compared to Fig. 5(D)). The ectodermal localization is clearly visible in the side view (Fig. 4(G)) and in Fig.4 (H) depicting a detail of the basal disc. The transgene was localized in the cytosol as well as the membranes (similar to Fig. 5(G)). Whether effects of the integration site or regulatory elements within the FGFR coding sequence cause this pattern, was not further investigated.

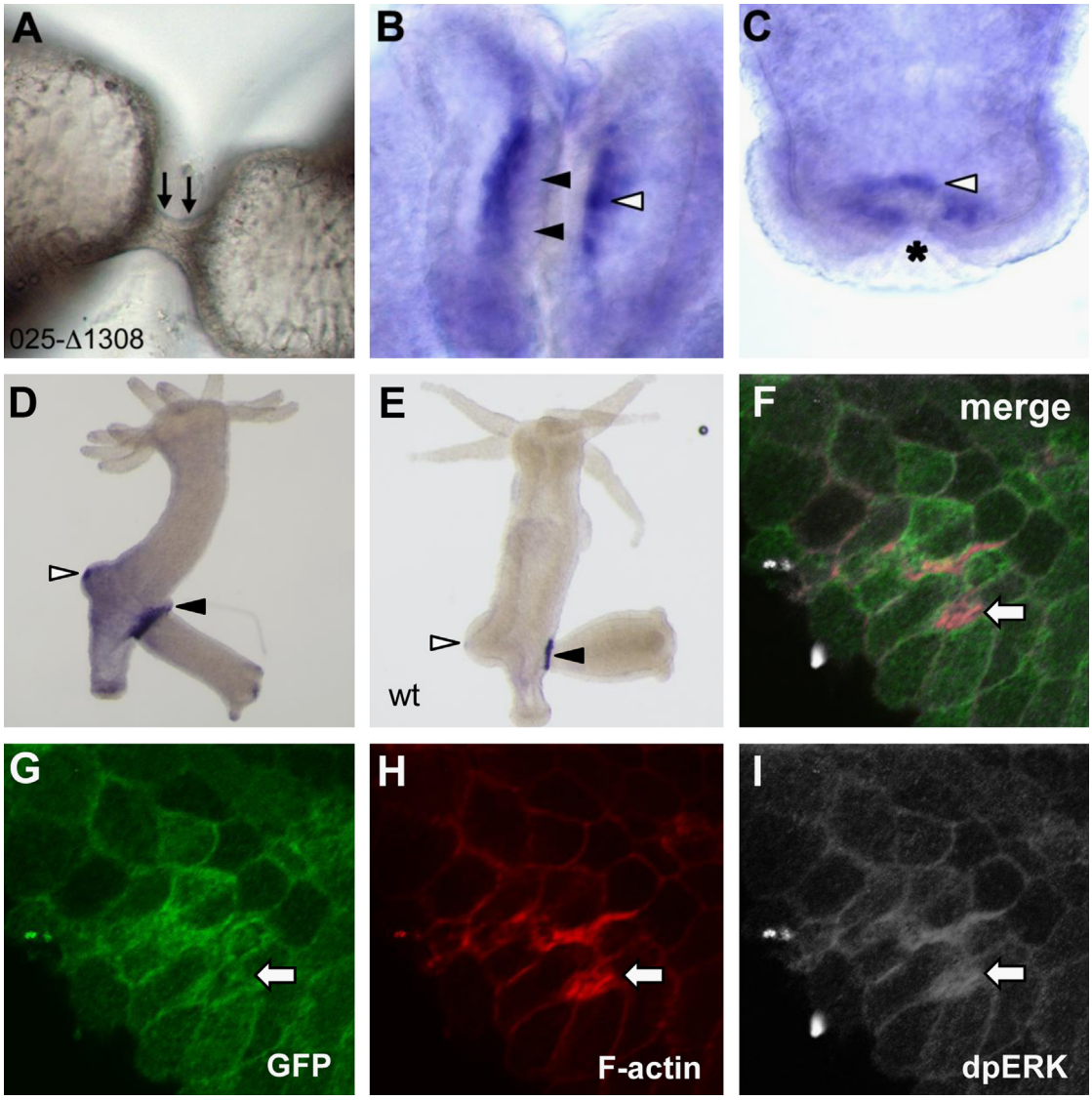

Fig. 5. Expression pattern of *kringelchen* and localization of GFP, dpERK and F-actin in the *025-kringΔ1308-GFP* line. (A) Close-up of the tissue bridge (arrows) between parent and nondetaching bud under light microscopy. (B) and (C) In situ hybridization of such a polyp with the *kringelchen* probe. Ectodermal expression (black arrowhead), endodermal (white arrowhead). (C) This polyp was separated mechanically from its parent, ectopic expression is detectable in the bud endoderm close to the basal pore (asterisk). (D) In situ hybridization of a budding *KringΔ1308-GFP* polyp. Additional to the normal *kringelchen* expression domains in the early bud hypostome and in the ring at the stage 6 bud base, the transgene is also detectable weakly throughout the lower body region and in the parent's basal disc. (E) Wildtype polyp showing *kringelchen* expression restricted to the early bud tip and stage 7 bud base. (F)–(H) Triple labeling for, dpERK and F-actin (by phalloidin). (F) overlay of G, H and I, (G) Localization of *Kring Δ1308-GFP* in the cell membrane and cytosol (arrow). (H) F-actin partially colocalizes *KringΔ1308-GFP* positive cells, (I) Only a very weak dpERK signal was detected in cells expressing the dominant-negative FGFR (shown in a strongly enhanced picture, a single dpERK-positive nucleus is seen on the left).

Animals carrying *kringΔ1308-GFP* at first glance developed normal. Immediately prior to bud detachment, however, development stopped. The young polyps remained attached to the parent yielding a colony-like phenotype (Fig. 4(B), (C), and (F)). All young polyps had formed an apparently normal basal disc (Fig. 4(G) and (H)), but remained connected to the parent with a thin tissue bridge containing ecto- and endodermal cells (compare Fig. 5(A)). To our knowledge, such a phenotype has not been described before. Detection of peroxidase activity (Hoffmeister and Schaller, 1985) in the basal discs of such a bud verified that it had acquired this typical biochemical marker for a mature basal discs (not shown), a double labeling using an antibody against GFP did not yield convincing results.

Young polyps, in which less than one third of the basal disc expressed the transgene (Fig. 4(H)), were able to detach although delayed for up to one week. All others persisted and were transported towards the basal disc by normal tissue movement and released about 6 weeks later. The phenotype occurred in those partially transgenic animals only, which expressed the transgene mainly in the lower body region (Fig. 5(D)). Normally, *kringelchen* is not expressed in the body column between two evaginating buds (Fig. 5(E)).

In contrast to normal buds (Fig. 2(M) and (N)), these *kringΔ 1308-GFP* polyps showed persistent ectopic *kringelchen* expression in the ecto- as well as the endoderm of the late bud basal disc (Fig. 5(B) and (C)). Since all the *kringΔ1308-GFP* lines carry the transgene ectodermally (compare Fig. 4), the ectopic endodermal signal visible in Fig. 5(B) and (C) must have been caused by endogenous *kringelchen*. The normal *kringelchen* expression domains in the apical tip of stage 3–4 buds and from stage 4 onwards in a ring at the bud base were unchanged (Fig. 5(D), Fig. 2(E) and (K)). Thus, *kringΔ1308-GFP* does not interfere with

sites of normal transcription, but allows (or induces) ectopic endodermal expression of the endogenous *kringelchen* in the basal disc. This potential cross-regulation is interesting and has to be investigated in the future in more detail.

We next investigated whether the dpERK-positive cluster forms despite knockdown by the dominant-negative FGFR. Triple labeling for GFP (detecting the transgene KringΔ1308-GFP), dpERK and TRITC-phalloidin was carried out. We included the TRITC-phalloidin staining to detect F-actin, because tissue constriction requires rearrangement of the actin cytoskeleton. In the thin tissue bridge connecting non-detaching polyps and parent, KringΔ1308-GFP was detected in the cell membrane of epithelial cells (Fig. 5 (G)). A dpERK-positive cluster was undetectable (Fig. 5(I)). In some of the Kring-Δ 1308-GFP cells carrying the transgene in the cell membrane and the cytoplasm, F-actin had, in fact, accumulated (Fig. 5(F) and (H) arrow).

Ectopic expression of the transgene in extended areas of a polyp (Fig. S5 (A) and (B)) altered bud morphogenesis and suppressed formation of a basal constriction similar to SU5402 treatment (Fig. S5(C)–(E)). The young polyps persisted as secondary axes connected to the parent by a broad tissue bridge. In these polyps, the actin cytoskeleton was massively disorganized at the branching border (Fig. S5(D) and (E) compared to a normal bud region (F) and (G)). Normally, the actin fibers of the ectodermal

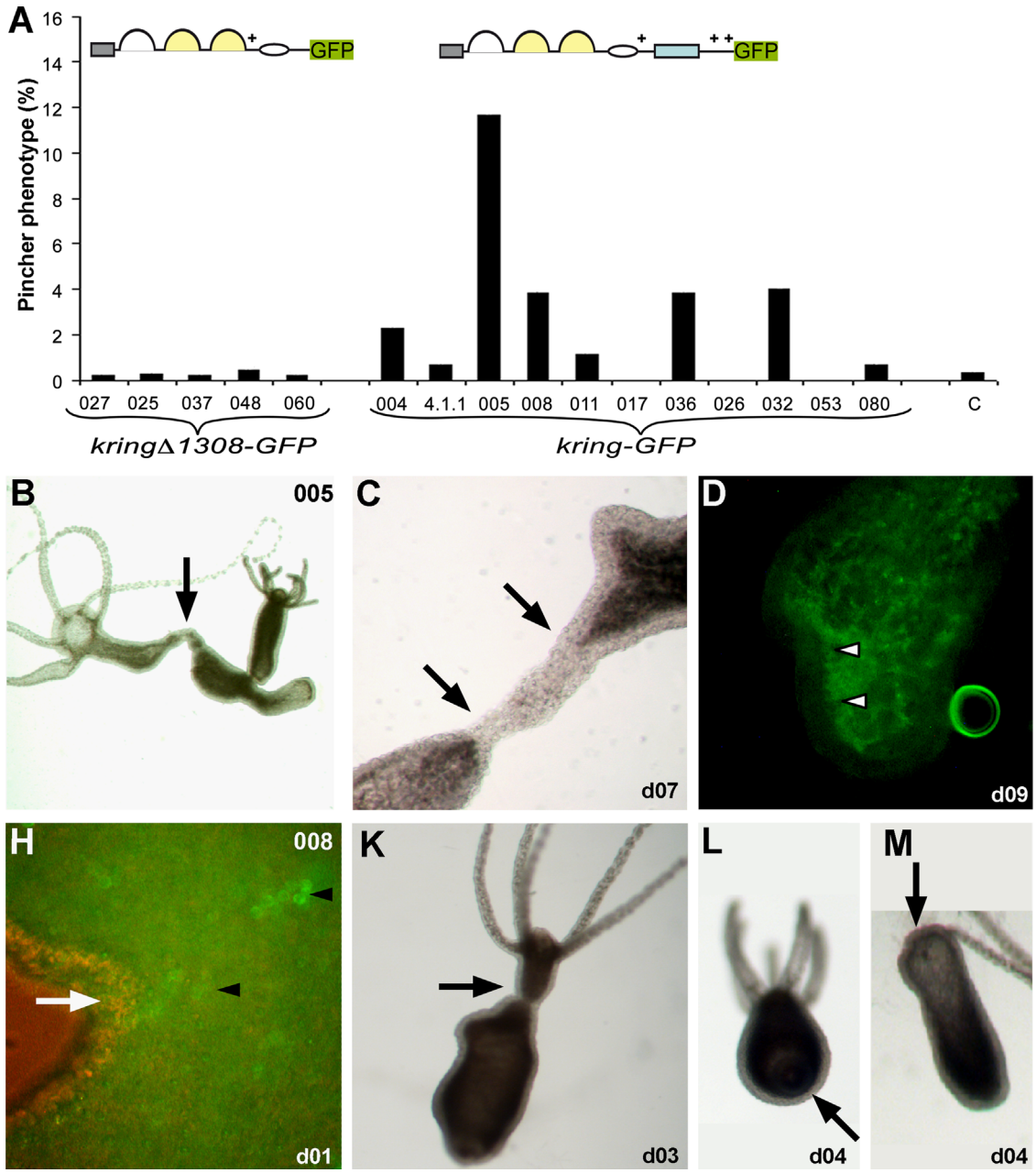

Fig. 6. *Kring-GFP* transgenic lines develop a pincher phenotype: the body column undergoes autotomy. (A) Percentage of the pincher phenotype occurring in *kring-GFP* polyps compared to nontransgenic *Hydra* and *kringΔ1308-GFP* lines—evaluation was bi-weekly over about one year. Presence of the transgene was verified by PCR. (B)–(D) line 005. (D). (B) Animal on day 5 of constriction (arrowhead) formation, (C) on day 7, when the endoderm has already separated (black arrowheads) and (D) upper tissue fragment following complete tissue separation on day 9. Line 005 expressed the transgene in a patchy pattern, separation occurred at a patch of cells with stronger expression (white arrows). (H)–(M) line 008 showed ectodermal expression of the transgene. (H) Life imaging, arrows indicate Kring-GFP-positive cells in the living animal, the arrowhead points to the constriction. (K) A constriction has formed within 3 days, (L,M) separated tissue pieces on day 4. Indicated in the lower right corner are the days after the first occurrence of a constriction.

epitheliomuscular cells run longitudinally, the endodermal ones circular. The chaotic arrangement of actin fibers at the intersection between parent and bud (Fig. S5(E)) indicates that FGFR is very likely essential in *Hydra* to establish a normally arranged actin cytoskeleton.

From the results obtained with the dominant-negative *Hydra* lines, we conclude that attenuated FGFR signaling (by the truncated FGFR) in the lower gastric column does not interfere with formation of a normal basal disc in the young polyp. However, it prevents removal of the thin tissue bridge between parent and bud. Correlation with the lack of the dpERK-positive cluster indicates a direct effect of FGFR on ERK phosphorylation. Furthermore, the data suggest that FGFR signaling controls formation of the constriction by a pathway targeting the actin cytoskeleton.

Locally restricted ectopic Kringelchen induces tissue separation and F-actin rearrangement in epitheliomuscular cells

The above results raised the question whether ectopic expression of the full length Kringelchen FGFR is able to induce dpERK and affect budding.

We therefore established *Hydra* lines transgenic for the full length, GFP-tagged FGFR (*kring-GFP*). Of twelve resulting transgenic lines, only two were stable for about 1 year, lines *kring-GFP-005* and *kring-GFP-008*. In most others, strong local expression of Kring-GFP was accompanied by formation of patchy tumour-like piles of the GFP-positive cells (Fig. S6), which were mechanically unstable and disintegrated when touched by a needle or a brine shrimp.

Line *kring-GFP-005* expressed the transgene in endodermal cells, line *kring-GFP-008* in ectodermal cells (Fig. 6(D) and (H) and compare Fig. S4). The phenotype of non-detaching buds with a fully developed foot described for *kringΔ1308-GFP* did not occur (Fig. 6(A)), but buds expressing the transgene in extended body regions failed to form a basal constriction (not shown, but similar to Fig. S5(A) and (B)). This phenotype indicates that unbalanced FGFR signaling (either up- or downregulated) interferes with formation of a constriction at the bud base.

The main phenotype of ectopic expression was autotomy of the polyps (Fig. 6). Besides normal bud detachment, the *kring-GFP* lines developed a single transversal constriction running across the parent's body column (neither close to the apical nor the basal end) and finally the tissue separated resulting in an isolated upper and lower body region (Fig. 6(B) and (C) and (H)–(M)). The fragments regenerated the missing head and foot structures within one week, and two small, apparently normal polyps resulted.

The pincher phenotype occurred only in partially transgenic animals and in waves taking about 2 months followed by a quiescent phase. In peak times up to 40% of the polyps developed a constriction in the body column and autotomized (summarized in Fig. 6(A).

Ecto- or endodermal expression of the transgene made a difference with respect to the speed of tissue separation (Fig. 6). Endodermal expression of *kringelchen-GFP* (in patches or transversal rows) induced tissue separation within about nine days (Fig. 6(B)–(D)). The endoderm always separated first (Fig. 6(C)), the nontransgenic ectoderm followed days later.

In contrast, ectodermal expression of Kring-GFP in cells arranged in a (not necessarily closed) transversal row of cells within nontransgenic tissue induced quick tissue separation within 4 days (Fig. 6(H) and (M)). This corresponds to about the time a bud needs for detachment.

The different speed of autotomy depending on ecto- or endodermal localization of Kringelchen-GFP indicates to a predominant role of the ectoderm in tissue separation and is consistent with the normally observed ectodermal expression of *kringelchen* (Sudhop et al., 2004).

A triple staining of Kringelchen-GFP, dpERK and F-actin in partially transgenic, early fragmenting polyps revealed in a surface view (Fig. 7(A), (C) and (E)) colocalization of ectodermal Kring-GFP and weak dpERK at and close to the site where the constriction started to form. Right at the constriction site, ectodermal cells were strongly compressed as seen by phalloidin staining (Fig. 7(A)). This compression might indicate transversal tension imposed to or generated by these cells. In fact, close to this site, the actin fibers in the basal processes of the ectodermal epitheliomuscular cells (Fig. 7(A) and (B)) deviate from their normal longitudinal direction and take a diagonal and finally almost circular direction. The normal arrangement of ectodermal cells is visible in the lower part of Fig. 7 (B), the normal circular arrangement of endodermal cells in the upper part of Fig. 7(B) (and compare to Fig. S5). In between, single actin bundles can be followed and their deviation from the normal longitudinal arrangement followed. These actin fibers are localized in the epitheliomuscular processes and probably act together with myosin.

Discussion

Budding in *Hydra* is an astonishing process in which, within four days, a complete young polyp forms by mass tissue movement from the parent and finally detaches. Preceding tissue separation, a sharp boundary between bud and parent is defined by crosstalk between FGFR and Notch signaling (Münder et al., 2010; Prexl et al., 2011; Sudhop et al., 2004). The establishment of this boundary is a prerequisite for the formation of a tissue constriction between bud and parent. How this constriction narrows to a thin tube and finally completes separation of the continuous, single layered ecto- and endodermal epithelia with their acellular extracellular matrix (ECM, mesogloea) is unknown.

Here, we provide evidence that initiation of the constriction and tissue separation directly depend on FGFR and, in the late phase, on FGFR/RAS/MEK/ERK signaling. We will discuss the role of FGFR (i) in formation of the constriction and (ii) in tissue separation and present a model (Fig. 8).

Ectodermal Kringelchen takes a leading role in formation of the constriction

From the transgenic *Hydra* expressing ectodermal Kringelchen-GFP ectopically, it is obvious, that ectodermal Kringelchen initiates formation of the constriction (Fig. 8(B)). Whenever the transgene is expressed in a row of cells in a nontransgenic environment, a transverse constriction forms and complete tissue separation of the *Hydra* body column occurs (Fig. 6).

Since the time course and ectodermal expression correspond to bud detachment, we consider bud detachment and autotomy as comparable processes which obey to similar rules. The fact that ecto- as well as the endodermal *kring-GFP* is able to induce autotomy, although at reduced speed in the latter case, suggests that the epithelia communicate (Fig. 8(F)). We propose that ectodermal signals via FGFR start the process and endodermal cells follow establishing a positive feedback loop. The endodermal signal(s) seem weaker or less effective than the ectodermal one(s). Potential candidates for this communication are FGFs, which may cross (or bind to) the extracellular matrix at different diffusion rates caused by their biochemical properties.

Our data provide evidence that fine tuning of FGFR signaling is required. Inhibition of FGFR as well as imbalanced Kringelchen signaling caused either by expression of *kring-Δ-1308-GFP* (Fig. S5)

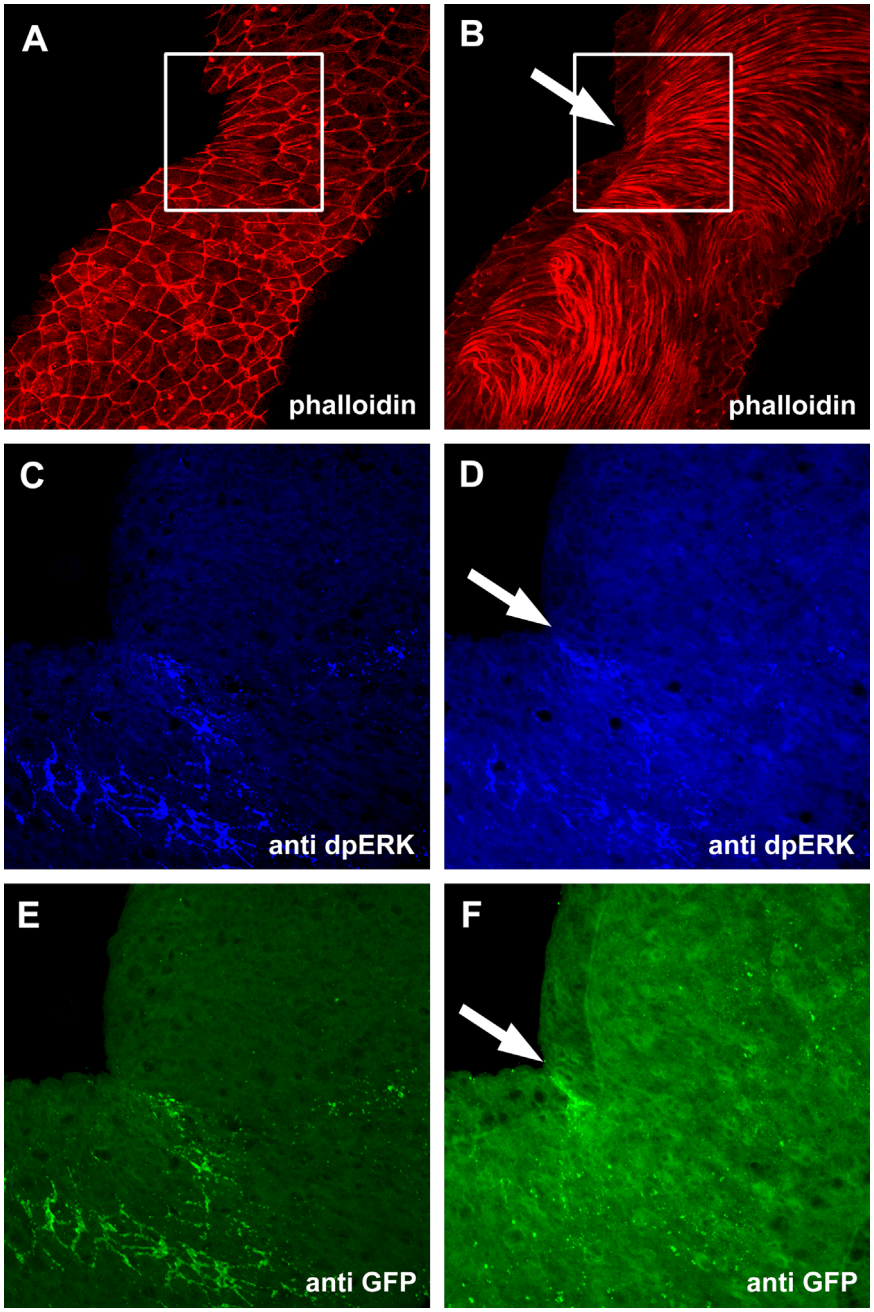

Fig. 7. Ectopic Kring-GFP correlates with dpERK and distorted actin fibers at a constriction site. Pictures were taken following triple detection of F-actin (by TRITC-phalloidin) (A) and (B), dpERK (C) and (D) and Kring-GFP (E) and (F). (A), (C), (E)) Optical section—surface level, (B), (D), (F)) optical section–deep level. (A) and (B)) F-actin was detected by phalloidin at the constriction site (arrowhead) of a polyp carrying the *kring-GFP* transgene. The actin cytoskeleton is strongly distorted close to the beginning constriction and ectodermal, longitudinal fibers converge towards the constriction site taking a transverse direction. The normal longitudinal orientation of ectodermal contractile fibers is retained only in the lower picture part, normal circular endodermal fibers are visible in the upper part. Phalloidin also stains punctuate structures of unknown nature.

or *kringelchen-GFP* in extended regions of the *Hydra* parent, all may prevent formation of the constriction. Interesting in this context is that attenuated Kringelchen signaling at the late bud of *kring-Δ-1308-GFP* animals (Fig. 4) does not interfere with formation of the constriction. Full morphogenesis of a basal disc is possible - provided the transgene is expressed in the lower body region. An interesting possibility which needs further investigation is that imported, nontransgenic tissue from the upper body region provides factors necessary for an almost normal development of a constriction up to the point, when detachment requires a strong input by a normal FGFR.

We propose a model in which ectodermal cells at the bud-parent boundary produce a signal, which is received by adjacent ecto- as well as endodermal cells (Fig. 8(F)). The endoderm might respond and stabilize the signal in a positive feedback loop. In further steps, we propose that the actin cytoskeleton is targeted and alters existing apical constrictions in ectodermal epitheliomuscular cells and basal constriction in their endodermal counterparts to the respective other direction (Fig. 8(D)). In order to close the bud's epithelia, basal constriction of ectodermal and apical constriction of endodermal cells is finally required with a leading role of the ectoderm.

An interesting candidate pathway for future investigation of the mechanisms leading to this constriction is the FGFR-RAS-RAC-RHO pathway. It is known from other systems to control apical constriction (Harding and Nechiporuk, 2012). It will also be

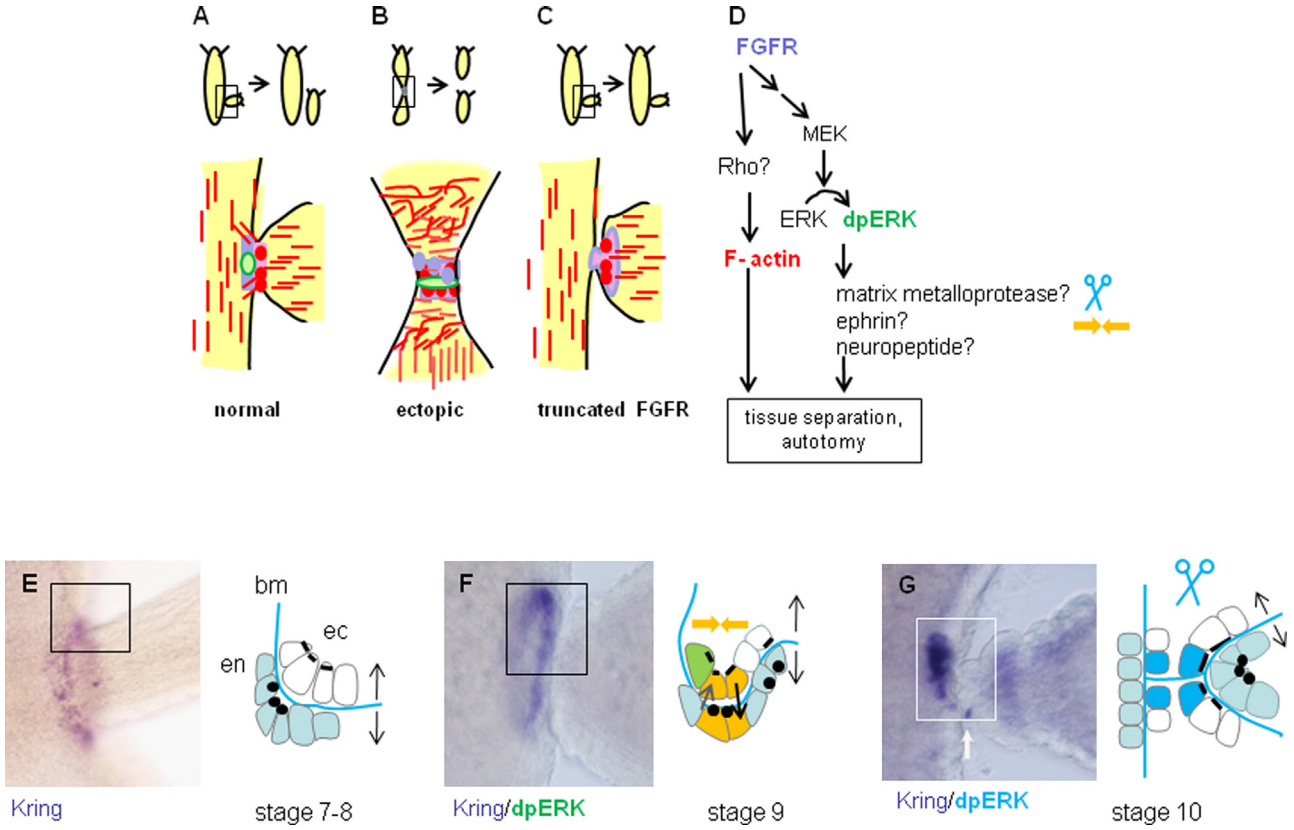

Fig. 8. Graphical summary and model scheme of FGFR-induced tissue separation in *Hydra* during normal budding, ectopic FGFR expression (Kring-GFP) and FGFR knockdown (KringΔ1308-GFP). FGFR-expressing cells (blue), cells putatively containing the protein (purple), F-actin in ectodermal epitheliomuscular cells (red), dpERK colocalized with FGFR (green). (A) Normal budding requires tissue separation associated with localized FGFR, generation of dpERK and F-actin (red). (B) Ectopic FGFR (Kring-GFP) induces autotomy of the body column associated with localized dpERK. F-actin fibers change their direction from longitudinal to circular directions adjacent to the separation site. (C) FGFR knockdown (KringΔ1308-GFP) prohibits bud detachment despite F-actin accumulation and is associated with lack of localized dpERK. (D) Model for FGFR downstream pathways and targets adressed in tissue separation. (E)–(G) Model for cell shape changes, putative signal centers and effectors of tissue separation in mid and late bud stages.

necessary to investigate myosin, which together with actin might be responsible for the strong elongation of cells revealed by TRITC-phalloidin staining at the constriction site of *kringelchen-GFP* polyps (Fig. 7).

Tissue separation depends on the activation of FGFR-ERK signaling

For the final phase of budding (and as well ectopic tissue separation), we propose that a second phase of FGFR activity activates ERK in cells at the boundary and within the tissue bridge. In our experiments, Kringelchen and dpERK colocalized in late buds and at ectopic separation sites. Moreover, pharmacological inhibition delayed bud detachment and prevented formation of the dpERK-positive cell cluster. The fact that dpERK was found in nuclei in successfully separating tissue indicates a direct function of dpERK. Nuclear dpERK is known to control transcription in vertebrates and fly, where 70% of the activated ERK are localized to nuclei (Lim et al., 2013).

Based on the functions that have to be fulfilled, several targets for transcriptional regulation are likely. The extracellular matrix between ecto-and endoderm has to be digested and separated in the tissue bridge, and in fact, the RNA encoding the matrix metalloproteases MMPA3 is coexpressed with Kringelchen at the bud base (Münder et al., 2010). For the final sphincter contraction, neuropeptides have to be and some of them are expressed in neurons close to the basal disc (Takahashi et al., 1997). Whether protease as well as peptide secretion require FGFR and activated ERK (Fig. 8(D)) are open questions and will be investigated in the future.

The biggest challenge for a complete separation of tissue between bud and parent, however, is separation of neighboring cells within the continuous epithelia. As a working hypothesis, we propose that this separation is effected by a switch from adhesive to antiadhesive properties of the neighbors. Highly interesting candidate proteins to establish antiadhesive properties are ephrins and their receptors. They are known as bidirectionally acting molecules with many functions including targeting of the cytoskeleton and senescence of cells (Pasquale, 2008). Of particular interest for *Hydra* budding is their action in circulatory systems, where they keep veins and arteries apart, but allow fusion of both in the capillary bed to form anastomoses (for a review see (Patel-Hett and D'Amore, 2011). An inverse process might occur in *Hydra*, where an anastomose-like continuous tube connects parent and bud, and has to be closed to yield two independent animals (Fig. 8(F) (G)). Ephrins and their receptors have recently been described in *Hydra* (Tischer et al., 2013) and Ephrin-B1 is expressed at the bud base in late budding stages. Further analysis will show whether their expression is targeted by *Hydra* FGFR.

Conclusion

Polyps transgenic for either the full length or a putatively dominant-negative Kringelchen FGFR corroborate the hypothesis that tissue separation during *Hydra* budding critically depends on this FGFR. Ectopic expression of Kringelchen induces tissue separation within the polyp's body column, probably by a transient local activation of MEK-ERK signaling in a small cluster of

cells proximal to the separation site. The actin cytoskeleton is strongly affected in autotomizing polyps and thus, it seems to be another target for Kringelchen. Our study indicates a novel function of FGFR—not only in establishing a boundary between parent and young polyp (by Notch signaling) but in controlling the complete separation of continuous epithelia in a process inverse to the formation of anastomoses in circulatory systems.

Acknowledgements

We thank Arno Müller and Anna Klingseisen, Dundee, for advice on using the anti-dpERK antibody. Rob Steele and Robert Campbell kindly provided *Hydra vulgaris 1184A*. We are grateful to Anja Rudolf for help with the kLSM and Katja Gessner for graphics. Supported by the DFG Grant HA 1732-11.

Appendix A. Supplementary information

Supplementary data associated with this article can be found in the online version at http://dx.doi.org/10.1016/j.ydbio.2014.08.010.

References

Affolter, M., Zeller, R., Caussinus, E., 2009. Tissue remodelling through branching morphogenesis. Nat. Rev. Mol. Cell. Biol. 10, 831–842.
Amaya, E., Musci, T.J., Kirschner, M.W., 1991. Expression of a dominant negative mutant of the FGF receptor disrupts mesoderm formation in *Xenopus embryos*. Cell 66, 257–270.
Aufschnaiter, R., Zamir, E.A., Little, C.D., Ozbek, S., Munder, S., David, C.N., Li, L., Sarras Jr., M.P., Zhang, X., 2011. In vivo imaging of basement membrane movement: ECM patterning shapes Hydra polyps. J. Cell. Sci. 124, 4027–4038.
Chera, S., Ghila, L., Wenger, Y., Galliot, B., 2011. Injury-induced activation of the MAPK/CREB pathway triggers apoptosis-induced compensatory proliferation in hydra head regeneration. Dev. Growth Differ. 53, 186–201.
Cutaia, M., Davis, R., Parks, N., Rounds, S., 1996. Effect of ATP-induced permeabilization on loading of the Na^+ probe SBFI into endothelial cells. J. Appl. Physiol. 1985 (81), 509–515.
David, C.N., 1973. A quantitative method for maceration of *Hydra* tissue. Willielm Roux Arch. EntwMech. Org. 171, 259–268.
David, C.N., 2012. Interstitial stem cells in hydra: multipotency and decision-MAKING, Int. J. Dev. Biol. (in press).
David, C.N., Schmidt, N., Schade, M., Pauly, B., Alexandrova, O., Bottger, A., 2005. Hydra and the evolution of apoptosis. Integr. Comp. Biol. 45, 631–638.
Fabila, Y., Navarro, L., Fujisawa, T., Bode, H., Salgado, L., 2002. Selective inhibition of protein kinases blocks the formation of a new axis, the beginning of budding, in Hydra. Mech. Dev. 119, 157–164.
Harding, M.J., Nechiporuk, A.V., 2012. Fgfr-Ras-MAPK signaling is required for apical constriction via apical positioning of Rho-associated kinase during mechanosensory organ formation. Development 139, 3130–3135.
Hassel, M., Bridge, D., Stover, N., Kleinholz, H., Steele, R., 1998. The level of expression of a protein kinase C gene may be an important component of the patterning process in Hydra. Dev. Genes Evol. 207, 502–514.
Hemmrich, G., Anokhin, B., Zacharias, H., Bosch, T.C., 2007. Molecular phylogenetics in Hydra, a classical model in evolutionary developmental biology. Mol. Phylogenet. Evol. 44, 281–290.
Hobmayer, B., Jenewein, M., Eder, D., Eder, M.K., Glasauer, S., Gufler, S., Hartl, M., Salvenmoser, W., 2012. Stemness in Hydra—a current perspective. Int. J. Dev. Biol. 56, 509–517.
Hobmayer, B., Rentzsch, F., Kuhn, K., Happel, C., von Laue, C., Snyder, P., Rothbächer, U., Holstein, T., 2000. WNT signaling molecules act in axis formation in the diploblastic metazoan Hydra. Nature 407, 186–189.
Hoffmeister, S.A.H., Schaller, H.C., 1985. A new biochemical marker for foot-specific differentiation in hydra. Roux Arch Dev Biol. 194, 453–461.
Holstein, T.W., Hobmayer, E., David, C.N., 1991. Pattern of epithelial cell cycling in hydra. Dev. Biol. 148, 602–611.
Kadam, S., Mc Mahon, A., Tzou, P., Stathopoulos, A., 2009. FGF ligands in Drosophila have distinct activities required to support cell migration and differentiation. Development 136, 739–747.
Kaloulis, K., Chera, S., Hassel, M., Gauchat, D., Galliot, B., 2004. Reactivation of developmental programs: the cAMP-response element-binding protein pathway is involved in hydra head regeneration. Proc. Natl. Acad. Sci. USA 101, 2363–2368.
Khalturin, K., Anton-Erxleben, F., Milde, S., Plotz, C., Wittlieb, J., Hemmrich, G., Bosch, T.C., 2007. Transgenic stem cells in Hydra reveal an early evolutionary origin for key elements controlling self-renewal and differentiation. Dev. Biol. 309, 32–44.
Klingseisen, A., Clark, I.B., Gryzik, T., Muller, H.A., 2009. Differential and overlapping functions of two closely related Drosophila FGF8-like growth factors in mesoderm development. Development 136, 2393–2402.
Lemmon, M.A., Schlessinger, J., 2010. Cell signaling by receptor tyrosine kinases. Cell 141, 1117–1134.
Lim, B., Samper, N., Lu, H., Rushlow, C., Jimenez, G., Shvartsman, S.Y., 2013. Kinetics of gene derepression by ERK signaling. Proc. Natl. Acad. Sci. USA 110, 10330–10335.
Mandal, L., Dumstrei, K., Hartenstein, V., 2004. Role of FGFR signaling in the morphogenesis of the Drosophila visceral musculature. Dev. Dyn. 231, 342–348.
Manuel, G., Reynoso, R., Gee, L., Salgado, L., Bode, H., 2006. PI3K and ERK 1-2 regulate early stages during head regeneration in hydra. Dev. Growth Differ. 48, 129–138.
Martínez, D.E., Iñiguez, A.R., Percell, K.M., Willner, J.B., Signorovitch, J., Campbell, R.D., 2010. Phylogeny and biogeography of Hydra (Cnidaria: Hydridae) using mitochondrial and nuclear DNA sequences. Mol. Phylogenet. Evol. 57, 403–410.
Muha, V., Muller, H.A., 2013. Functions and mechanisms of fibroblast growth factor (FGF) signaling in *Drosophila melanogaster*. Int. J. Mol. Sci. 14, 5920–5937.
Müller, W., 1989. Diacylglycerol-induced multihead formation in Hydra. Development 105, 306–316.
Münder, S., Käsbauer, T., Prexl, A., Aufschnaiter, R., Zhang, X., Towb, P., Böttger, A., 2010. Notch signaling defines critical boundary during budding in Hydra. Dev. Biol. 344, 331–345.
Otto, J., Campbell, R., 1977. Budding in Hydra attenuata: bud stages and fate map. J. Exp. Zool 200, 417–428.
Pasquale, E.B., 2008. Eph-ephrin bidirectional signaling in physiology and disease. Cell 133, 38–52.
Patel-Hett, S., D'Amore, P.A., 2011. Signal transduction in vasculogenesis and developmental angiogenesis. Int. J. Dev. Biol. 55, 353–363.
Philipp, I., Aufschnaiter, R., Ozbek, S., Pontasch, S., Jenewein, M., Watanabe, H., Rentzsch, F., Holstein, T.W., Hobmayer, B., 2009. Wnt/beta-Catenin and non-canonical Wnt signaling interact in tissue evagination in the simple eumetazoan Hydra. Proc. Natl. Acad. Sci. USA 106, 4290–4295.
Prexl, A., Munder, S., Loy, B., Kremmer, E., Tischer, S., Bottger, A., 2011. The putative Notch Ligand HyJagged is a transmembrane protein present in all cell types of adult hydra and upregulated at the boundary between bud and parent. BMC Cell Biol. 12, 38.
Rebscher, N., Deichmann, C., Sudhop, S., Fritzenwanker, J., Green, S., Hassel, M., 2009. Conserved intron positions in FGFR genes reflect the modular structure of FGFR and reveal stepwise addition of domains to an already complex ancestral FGFR. Dev Genes Evol. 219, 455–468.
Rentzsch, F., Fritzenwanker, J., Scholz, C., Technau, U., 2008. FGF signaling controls formation of the apical sensory organ in the cnidarian Nematostella vectensis. Development 135, 1761–1769.
Rottinger, E., Saudemont, A., Duboc, V., Besnardeau, L., McClay, D., Lepage, T., 2008. FGF signals guide migration of mesenchymal cells, control skeletal morphogenesis [corrected] and regulate gastrulation during sea urchin development. Development 135, 353–365.
Rudolf, A., Hübinger, C., Hüsken, K., Vogt, A., Rebscher, N., Onel, S.F., Renkawitz-Pohl, R., Hassel, M., 2012. The Hydra FGFR, Kringelchen, partially replaces the Drosophila Heartless FGFR. Dev Genes Evol.
Sanmartin-Suarez, C., Soto-Otero, R., Sanchez-Sellero, I., Mendez-Alvarez, E., 2011. Antioxidant properties of dimethyl sulfoxide and its viability as a solvent in the evaluation of neuroprotective antioxidants. J. Pharmacol. Toxicol. Methods 63, 209–215.
Sudhop, S., Coulier, F., Bieller, A., Vogt, A., Hotz, T., Hassel, M., 2004. Signaling by the FGFR-like tyrosine kinase, Kringelchen, is essential for bud detachment in *Hydra vulgaris*. Development 131, 4001–4011.
Takahashi, T., Muneoka, Y., Lohmann, J., Lopez de Haro, M., Solleder, G., Bosch, T., David, C., Bode, H., Koizumi, O., Shimizu, H., Hatta, M., Fujisawa, T., Sugiyama, T, 1997. Systematic isolation of peptide signal molecules regulating development in hydra: LWamide and PW families. Proc. Natl. Acad. Sci. USA 94, 1241–1246.
Tischer, S., Reineck, M., Soding, J., Munder, S., Bottger, A., 2013. Eph receptors and ephrin class B ligands are expressed at tissue boundaries in *Hydra vulgaris*. Int. J. Dev. Biol. 57, 759–765.
Weber, J., 1995. Novel tools for the study of development, migration and turnover of nematocytes (cnidarian stinging cells). J. Cell. Sci. 108 (Pt 1), 403–412.
Wittlieb, J., Khalturin, K., Lohmann, J., Anton-Erxleben, F., Bosch, T., 2006. Transgenic Hydra allow in vivo tracking of individual stem cells during morphogenesis. Proc. Natl. Acad. Sci. USA 103, 6208–6211.
Zar, J.H. (2010) Biostatistical analysis. Fifth edition. Prentice-Hall/Pearson.